ELSEVIER

Journal of Organometallic Chemistry 654 (2002) 8–15

Journal of Organometallic Chemistry

www.elsevier.com/locate/jorganchem

Alkoxycarbonyl substituted ruthenium mono(bipyridine) complexes: steric effects of the bipyridine substituents

Toni-J.J. Kinnunen, Matti Haukka *, Tapani A. Pakkanen

Department of Chemistry, University of Joensuu, P.O. Box 111, FIN-80101 Joensuu, Finland

Received 21 November 2001; received in revised form 12 February 2002; accepted 15 February 2002

Abstract

Mono(bipyridine) complexes of ruthenium (n,n'-L_2-2,2′-bpy)$Ru(CO)_2Cl_2$ ($n = 3$, 4, 5, or 6; L = CO(O)Me or CO(O)Et) were synthesised and structurally characterised. The steric effects of the substituents L on the geometry and the energetics of the compounds were studied using both experimental and theoretical methods to clarify the effect of substituent position on complex behaviour and electrochemical properties. Calculations were carried out with the density functional hybrid B3PW91 method. The position of the substituent was found to strongly effect the geometry and the energy of the mono(bipyridine) complexes. Alkoxycarbonyl substituents at 3,3′- and 6,6′-positions caused strong structural distortion of the complexes. The strain caused by 6,6′-substituents was readily relaxed forming new chelating complex with tridentate ligand coordination. Varying the bipyridine substituent position also caused changes in the electrochemical properties of the compounds reflected by the variations in the HOMO–LUMO energy gap. Ligand modifications caused by changing the substituent locations offer possibilities to design complexes with the required structural or electrochemical properties. © 2002 Elsevier Science B.V. All rights reserved.

Keywords: Mono(bipyridine) complexes; Steric effects; Alkoxycarbonyl substitutents

1. Introduction

Transition metal complexes containing polydentate nitrogen donor ligands are widely studied and used in different contexts. Like transition metal complexes in general, compounds with nitrogen ligands have, for example, been applied in several catalytic reactions. Bipyridine complexes [1,2] of ruthenium are well-known catalysts for the water gas shift reaction (WGSR) in both homo- and heterogeneous processes. Polymerisation of α-olefins catalysed by transition metal compounds with nitrogen-ligands has also been of interest during the last decade. Nickel and palladium amino complexes have proven to be active and selective catalysts in polyolefin synthesis [3].

The structural properties of the bipyridine ligand, i.e. the presence of substituents and their location in the ring system, strongly affect the catalytic properties of bipyridine complexes, for example, in the WGSR [4]. The catalytic activity of n,n'-dimethyl-2,2′-bipyridine complexes have found to be dependent on the position of the methyl substituent. Steric hindrance of the ruthenium centre caused by methyls at 6,6′-positions led about 90% less active catalyst than in the case of 4,4′-dimethyl substituents. Similarly to WGSR, structural modifications of ligand have been reported to cause changes in catalytic activities in olefin polymerisation reactions [3,5].

Ruthenium bipyridines are widely utilised compounds in photo-electrochemical applications. The major advantages of ruthenium complexes in electrochemical applications are based on relatively low MLCT energy. In the case of ruthenium bipyridines MLCT mainly involves electron transfer from d-orbital of the metal centre to bipyridine π*-orbital. The electronic properties can be effectively manipulated by ligand exchanges and modifications. Variations in the ligand sphere induce changes in the electron density around the metal centre and, in turn, modify the electro- and photochemical properties of the ruthenium bipyridine complexes [6,7]. The tunability of the electronic properties can be

---

* Corresponding author. Fax: +358-13-2513390.
E-mail address: matti.haukka@joensuu.fi (M. Haukka).

0022-328X/02/$ - see front matter © 2002 Elsevier Science B.V. All rights reserved.
PII: S0022-328X(02)01224-X

utilised, for example, in designing complexes with required absorption properties.

In order to gain a deeper understanding of the steric effects of the bipyridine substituents on the properties of the complexes a systematic experimental and modelling study has been carried out. A series of new alkoxycarbonyl substituted bipyridine complexes of ruthenium has been synthesised and characterised. Variations in the position of the substituent on the bipyridine have been made. The modelling studies aim firstly at a reliable prediction of the energetics and geometries of the complexes. The second goal is to use modelling as a tool for designing ligands with desired properties. The dependence of the chemical and electrochemical properties of the ruthenium complexes on the ligands substitution will be discussed and shown to play a key role in the complex stability and reactivity.

2. Experimental

2.1. Materials and general procedures

Syntheses of the *n*,*n*′-dialkoxycarbonyl-2,2′-bipyridines were carried out according to the literature methods [8,9]. Mono(bipyridine) complexes of ruthenium, shown in Fig. 1, were synthesised from the substituted bipyridines and $[Ru(CO)_3Cl_2]_2$ (Alfa). All the commercially available reagents were used without further purification. Solvents were dried and deoxygenated prior to use. The FT-IR spectra were measured with a Nicolet Magna-IR 750 spectrometer and the NMR spectra with a Bruker Digital NMR Avarice 250 MHz. Elemental analyses were carried out with EA1110 CHNS-O equipment (CE Instruments).

2.2. Syntheses

2.2.1. *cis-Cl-cis-CO-(4,4′-dimethoxycarbonyl-2,2′-bpy)RuCl₂(CO)₂ (**1**)*

The ligand (60 mg of 4,4′-dimethoxycarbonyl-2,2′-bipyridine), $[Ru(CO)_3Cl_2]_2$ (62 mg) and 3 ml of MeOH were introduced into a 100 ml Berghof autoclave equipped with a Teflon liner. The closed autoclave was rapidly heated to 120 °C and the reaction mixture was kept at this temperature for 5 h. The system was slowly (5 °C per hour) cooled to ambient temperature. The title compound was obtained as yellow crystals, which were characterised by single crystal X-ray diffraction. The yield of the product was very low, preventing further spectroscopic or elemental analysis.

2.2.2. *Trans-Cl-cis-CO-(4,4′-dimethoxycarbonyl-2,2′-bpy)RuCl₂(CO)₂ (**1b**)*

The MeOH solution of $[Ru(CO)_3Cl_2]_2$ (120 mg in 7 ml) was refluxed under nitrogen for 10 h followed by the addition of substituted bipyridine ligand (120 mg in 10 ml MeOH). The mixture was further refluxed for 18 h. A yellow product precipitated from a red solution. The precipitate was filtered, washed with MeOH and dried under vacuum. Yield: 152 mg (68%). Anal. Found: C, 38.29; H, 2.43; N, 5.59. Calc. for $C_{16}H_{12}Cl_2N_2O_6Ru$: C,

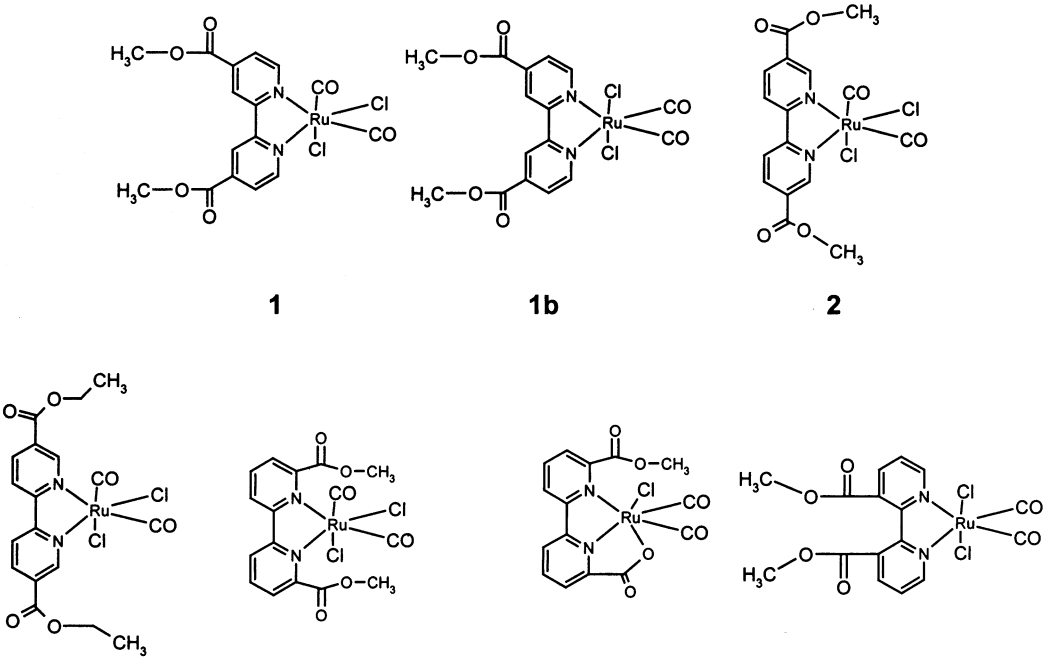
1 **1b** **2**

3 **4** **5** **6**

Fig. 1. Studied (*n*,*n*′-alkoxycarbonyl-2,2′-bpy)$RuCl_2(CO)_2$ complexes.

38.42; H, 2.42; N, 5.60%. IR (in CH_2Cl_2, cm^{-1}): 2068 and 2010 (CO). δ (250 MHz, $CDCl_3$) for bpy-ring 9.34 (d, 2H), 8.88 (s, 2H), 8.22 (d, 2H) and for –O–CH_3 4.11 (s, 6H).

2.2.3. *cis-Cl-cis-CO-(5,5′-dimethoxycarbonyl-2,2′-bpy)RuCl$_2$(CO)$_2$ (**2**)*

Complex **2** was synthesised by heating under reflux as described above. A green solid product was obtained from a dark red solution. Yield: 136 mg (61%). Anal. Found: C, 38.35; H, 2.50; N, 5.55. Calc. for $C_{16}H_{12}Cl_2N_2O_6Ru$: C, 38.42; H, 2.42; N, 5.60%. IR (in CH_2Cl_2, cm^{-1}): 2070 and 2010 (CO). δ (250 MHz, $CDCl_3$) for bpy-ring 8.41 (d, 2H), 9.73 (s, 2H), 8.70 (d, 2H) and –O–CH_3 4.08 (s, 6H).

2.2.4. *cis-Cl-cis-CO-(5,5′-diethoxycarbonyl-2,2′-bpy)RuCl$_2$(CO)$_2$ (**3**)*

The title compound was prepared similarly to complex **1b**. A yellowish–green solid product was filtered from the dark red solution. Yield: 134 mg (64%). Anal. Found: C, 40.63; H, 3.02; N, 5.29. Calc. for $C_{18}H_{16}Cl_2N_2O_6Ru$: C, 40.92; H, 3.05; N, 5.30%. IR (in CH_2Cl_2, cm^{-1}): 2069 and 2009 (CO). δ (250 MHz, $CDCl_3$) for bpy-ring 9.94 (d, 1H), 8.94 (d, 1H), 8.58 (d, 1H), 8.47 (d, 1H), 7.87 (d, 1H), 7.65 (d, 1H), for –O–CH_2– 3.81 (s, 4H) and for CH_3 1.57 (s, 6H).

2.2.5. *cis-Cl-cis-CO-(6,6′-dimethoxycarbonyl-2,2′-bpy)RuCl$_2$(CO)$_2$ (**4**)*

Because of the poor reactivity of the 6,6′-disubstituted bipy, a high temperature (120 °C) reaction in a closed vessel was used. The substituted bipyridine (50 mg), $[Ru(CO)_3Cl_2]_2$ (50 mg) and 3 ml of CH_2Cl_2 were introduced into the 100 ml Berghof autoclave equipped with a Teflon liner. The closed autoclave was rapidly heated to 120 °C and the reaction mixture was kept at this temperature for 4 h. The system was slowly (5 °C per hour) cooled to ambient temperature. The title compound was obtained as yellow crystals with very low yield. The low yield prevented a detailed NMR analysis, but the weak ^{1}H-NMR peak pattern in the aromatic region indicated a mixture of two components. Elemental analysis was in agreement with the ^{1}H-NMR results suggesting presence of ca. 1:1 mixture of complexes **4** and **5**. Anal. Found: C, 39.71; H, 2.34; N, 5.86. Calc. for $[C_{16}H_{12}Cl_2N_2O_6Ru]$–$[C_{15}H_9ClN_2O_6Ru]$: C, 39.19; H, 2.23; N, 5.90%. IR (in CH_2Cl_2, cm^{-1}): 2073 and 2014 (CO).

2.2.6. *cis-CO-(6-methoxycarbonyl-6′-carboxylate-2,2′-bipyridine)RuCl(CO)$_2$ (**5**)*

Synthesis was carried out in the same way as described above in the case of compound **4**, with the exception of the use of higher temperature (160 °C) and MeOH as solvent. The yield was low. Only a very few crystals of **5** were formed. IR (in CH_2Cl_2, cm^{-1}): 2073 and 2012 (CO). Because of the low yield no further spectroscopic analysis or reliable elemental analysis could be carried out.

2.3. *X-ray crystallography*

The X-ray diffraction data were collected on a Nonius KappaCCD diffractometer using Mo–K_α radiation ($\lambda = 0.71073$ Å) and a Collect [10] data collection program (**1**, **4** and **5**) or on a Nicolet R3m diffractometer using a ω-scan data collection mode and graphite monochromatised Mo–K_α radiation (**3**). For **3** the accurate cell parameters were obtained from 25 automatically centred reflections and the intensities were corrected for background and Lp factors. The DENZO and SCALEPACK [11] programs were used for cell refinements and data reduction for **1**, **4** and **5** and SHELXTL PLUS V. 4. [11,12] program package for **3**. The structures **1**, **3**, and **5** were solved by direct methods using the SHELXS-97 program [13] and the WinGX [14] graphical user interface. Structure **4** was solved by the Patterson method using the DIRDIF-99 program [15]. An empirical ψ-scan absorption correction was applied to **3** ($T_{max}/T_{min} = 0.156/0.129$). Structural refinements were carried out with the SHELXL-97 [16]. The hydrogens were placed in an idealised position and constrained to ride on their parent atom. The crystallographic data are summarised in Table 1. Selected bond lengths and angles together with the values for the optimised structures are shown in Table 2. The molecular structures of complexes **1** and **3**–**5** are presented in Figs. 2 and 3.

2.4. *Computational details*

The geometries of the complexes were optimised using the B3PW91 hybrid density functional method and employing 6-31G* as a basis set (for ruthenium: Huzinaga's extra basis 433321/4331/421) [17]. The B3PW91 was selected because it has found to be successful method in predicting the geometries and the energies of carbonyl containing ruthenium bipyridines [7,18]. Single point energies for the B3PW91 optimised structures were also calculated by the B3LYP method. The geometry optimisations were followed by a vibrational analysis. All calculations were carried out with the GAUSSIAN-94 program [18].

3. Results and discussion

The effect of the substituent location on the properties of the complex can be clearly seen when considering the energies of the optimised structures. Molecules with methoxy-substituents at the 4,4′- and 5,5′-positions of the bipyridine ring have much lower energy compared to

Table 1
Crystallographic data for complexes **1**, **3**–**5**

	1	**3**	**4**	**5**
Empirical formula	$C_{16}H_{12}Cl_2N_2O_6Ru$	$C_{18}H_{16}Cl_2N_2O_6Ru$	$C_{16}H_{12}Cl_2N_2O_6Ru$	$C_{15}H_9ClN_2O_6Ru$
Formula weight	500.25	528.30	500.25	449.76
T (K)	120(2)	293(2)	150(2)	150(2)
λ (Å)	0.71073	0.71073	0.71073	0.71073
Crystal system	Triclinic	Monoclinic	Triclinic	Monoclinic
Space group	$P\bar{1}$	$P2_1/c$	$P\bar{1}$	$P2_1/c$
a (Å)	7.0670(2)	15.269(4)	7.75650(10)	7.7919(1)
b (Å)	12.0543(3)	9.694(2)	8.7893(2)	12.5020(3)
c (Å)	12.3182(4)	15.710(3)	13.4945(3)	15.8829(3)
α (°)	61.305(1)	90	100.166(1)	90
β (°)	87.641(1)	109.35(2)	94.534(1)	90.424(1)
γ (°)	74.895(2)	90	99.651(1)	90
V (Å^3)	884.30(4)	2194.2(9)	887.11(3)	1547.18(5)
Z	2	4	2	4
D_{calc} (g cm^{-3})	1.879	1.599	1.873	1.931
μ (mm^{-1})	1.226	0.993	1.222	1.223
Reflections collected	7539	3966	7649	6550
Unique reflections	3963	3817	3984	3401
R_{int}	0.0293	0.0467	0.0129	0.0246
R_1 [a]	0.0384	0.0559	0.0246	0.0273
wR_2 [a]	0.0773	0.1079	0.0598	0.0639

[a] $I \geq 2\sigma$.

the compounds with substituents at the 3,3′- or 6,6′-positions (Table 3 and Fig. 4). The geometric strain causes this energy increase; normally the nearly planar bipyridine system is bent and the ruthenium atom has positioned off the bipyridine-plane (Table 4 and Fig. 5). In a typical planar system the torsion angle C13–C14–C15–C16 is nearly zero. In the 3,3′-substituted complex **6** the corresponding value of 35° deviates considerably from zero. Similar distortion can also be found in 6,6′-substituted complex **4** although the deviation is less enhanced. In this case the torsion angle is about 12°. More than off-plane distortion of the two rings, the

Table 2
Experimental and calculated bond lengths (Å) and angles (°) of complexes **1**, **3**–**5**

	Complex **1**		Complex **3**		Complex **4**		Complex **5**	
	Experimental	Calculated	Experimental	Calculated	Experimental	Calculated	Experimental	Calculated
Bond lengths								
Ru–N1	2.111(3)	2.147	2.075(5)	2.110	2.111(6)	2.141	2.002(2)	2.030
Ru–N2	2.074(3)	2.100	2.113(7)	2.150	2.148(5)	2.200	2.109(2)	2.200
Ru–C1	1.970(4)	1.880					1.916(3)	1.910
Ru–C2			1.865(1)	1.880	1.894(2)	1.870		
Ru–C3	1.911(4)	1.880	1.858(9)	1.880	1.875(2)	1.880	1.876(3)	1.880
Ru–C11	2.414(1)	2.420	2.399(2)	2.430	2.436(6)	2.450	2.402(3)	2.420
Ru–C13	2.391(0)	2.410	2.397(2)	2.410	2.388(1)	2.400		
Ru–O612							2.091(5)	2.080
C61–O612							1.301(3)	1.300
C1–O1	1.036(4)	1.140					1.132(3)	1.140
C2–O2			1.149(1)	1.140	1.108(3)	1.140		
C3–O3	1.104(5)	1.150	1.129(9)	1.150	1.135(3)	1.140	1.134(3)	1.150
Bond angles								
N1–Ru–N2	77.8(1)	77.3	78.9(2)	77.2	77.8(7)	77.0	79.0(1)	77.3
C1–Ru–C3	89.9(4)	93.3					94.0(2)	93.3
C2–Ru–C3			91.5(3)	93.2	89.7(5)	92.9		
C11–Ru–C13	91.2(2)	92.8	90.9(6)	92.8	87.2(1)	90.4		
Ru–C1–O1	172.4(3)	178.44					174.9(2)	176.1
Ru–C2–O2			176.8(7)	178.6	178.4(4)	177.5		
Ru–C3–O3	174.0(3)	179.45	178.5(7)	179.5	176.5(2)	178.6	176.1(2)	179.2

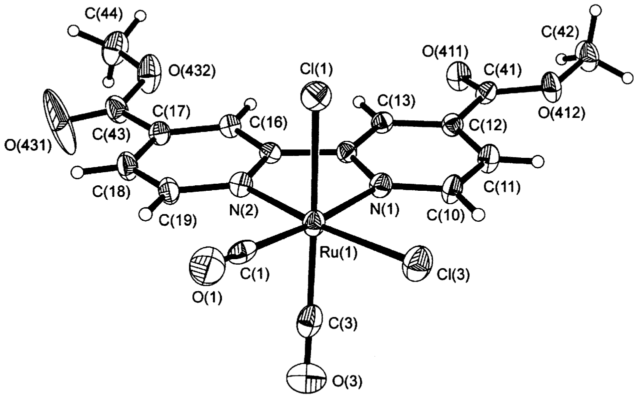

1

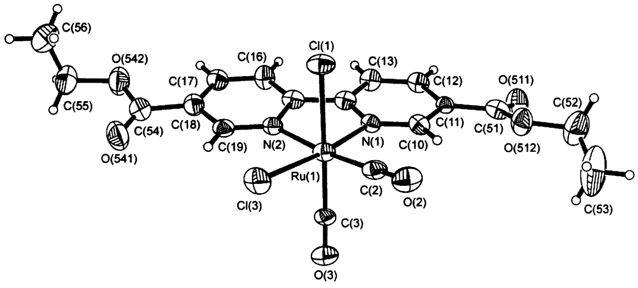

3

Fig. 2. X-ray crystal structures of complexes **1** and **3**. The thermal ellipsoids are drawn at the 50% probability level.

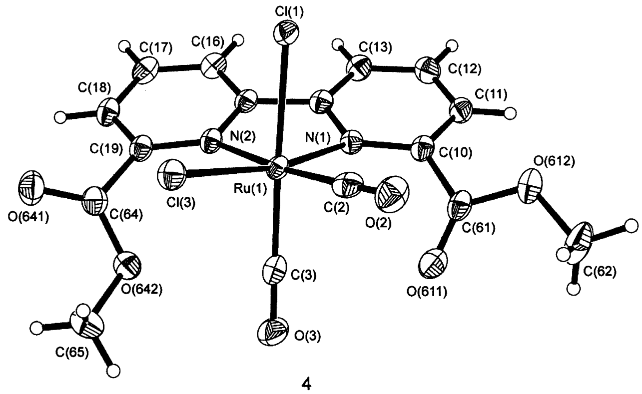

4

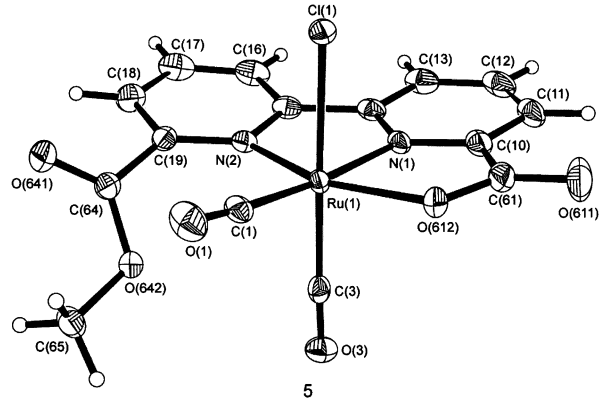

5

Fig. 3. X-ray crystal structures of complexes **4** and **5**. The thermal ellipsoids are drawn at the 50% probability level.

alkoxycarbonyl substituents at 6,6′-positions cause ruthenium to bend off the bipy-plane, as it can be seen in Fig. 5. The latter have stronger effect on the relative energy of the complex.

The 3,3′-substituted complex **6** seems energetically to be slightly more favourable than the 6,6′-substituted complex **4**. Despite the more unfavourable energetics, a stabile complex **4** can be synthesised and isolated. An elevated temperature of 120 °C and a closed reaction system were required to obtain this compound; the formation of other alkoxycarbonyl substituted complexes were achieved under reflux in methanol. When an even higher reaction temperature of 160 °C was used, the crystalline compound **5** with non-symmetric tridentate *N*,*N*,*O* coordination (Fig. 3) could be isolated. The detailed chelation route is not known, but it most probably proceeds via the cleavage of methyl chloride. Analysis of the products indicated some formation of **5** already in 120° producing the mixture of compounds **4** and **5**, while the increase of reaction temperature from 120 to 160 °C drives the equilibrium toward the chelate structure. The chelating procedure is understandable because of steric strain in **4**. The tridentate coordination in **5** to metal relaxes the distortion forming complex with the structure when the ruthenium centre is located on a bipyridine plane. The possibility to tridentate coordination in complex **4** shows the key role of the substituent position on the stability of the complex.

Table 3
The relative energies of the optimised (*n*,*n*′-methoxycarbonyl-2,2′-bpy)$RuCl_2(CO)_2$ complexes

Isomer	*n*,*n*′	$E-E_0$ (kJ mol^{-1})	
		B3PW91	B3LYP
trans(Cl)	3,3′	65.24	63.52
trans(Cl)	4,4′	0 [a]	0 [a]
trans(Cl)	5,5′	−0.77	−1.36
trans(Cl)	6,6′	78.14	73.10
cis(Cl)	3,3′	66.80	68.19
cis(Cl)	4,4′	0.02	3.33
cis(Cl)	5,5′	4.21	7.99
cis(Cl)	6,6′	69.50	68.26

[a] The energy of *trans*-Cl-(4,4′-dimethoxy-2,2′-bpy)$RuCl_2(CO)_2$ set to be the reference value E_0.

Photo-electrochemical properties of the metal complexes can be related to the energy differences between the highest occupied and lowest unoccupied molecular orbital. Our earlier results of 4,4′-substituted bipyridine complexes showed a linear trend between the absorption maximum and HOMO–LUMO gap [7]. The energy

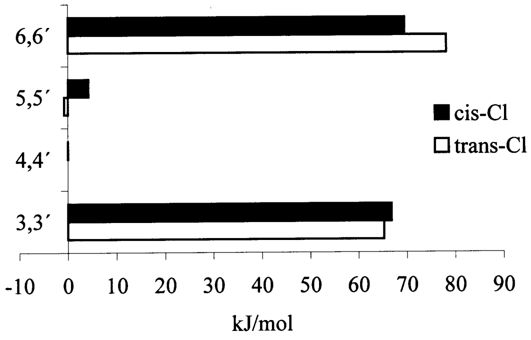

Fig. 4. The relative energies of the optimised (*n*,*n*′-alkoxycarbonyl-2,2′-bpy)RuCl$_2$(CO)$_2$ complexes.

Table 4
Torsion angles of *cis*-Cl-*cis*-CO-(3,3′-dimethoxycarbonyl-2,2′-bipy)RuCl$_2$(CO)$_2$ and *cis*-Cl-(6,6′-dimethoxycarbonyl-2,2′-bipy)RuCl$_2$(CO)$_2$

Angle (°)	3,3′-Disubstituted	6,6′-Disubstituted
C13–C14–C15–C16	35.0	11.7
N1–C14–C15–N2	29.0	11.0
C11–C10–N1–Ru	156.7	165.0
C18–C19–N2–Ru	166.7	148.2

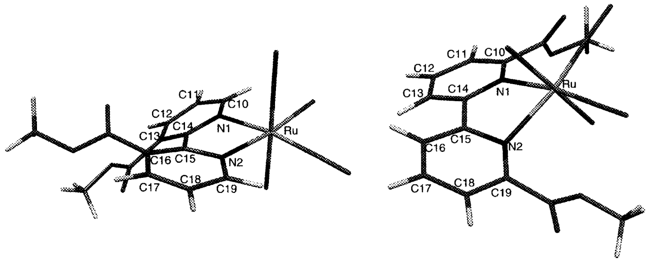

Fig. 5. Optimised structures of *cis*-Cl-*cis*-CO-(3,3′-dimethoxycarbonyl-2,2′-bipy)RuCl$_2$(CO)$_2$ and *cis*-Cl-*cis*-CO-(6,6′-dimethoxycarbonyl-2,2′-bipy)RuCl$_2$(CO)$_2$.

difference between HOMO and LUMO was shown to be adjustable by the electronic character of the substituents. Alkoxycarbonyl substituents are electron-withdrawing groups. In the case of complex **1b**, methoxycarbonyl substituents at 4,4′-positions decrease the HOMO–LUMO difference compared with the values of the unsubstituted (2,2′-bpy)RuCl$_2$(CO)$_2$. For complex **1b** the predicted energy difference estimated on the base of our earlier results [7] and the observed $\lambda_{\max}$ of 376 nm, is 2.74 eV, which is in good agreement with the energy gap of 2.78 eV obtained by DFT calculations. The DFT energy differences and the IR data of the complexes are summarised in Table 5. As shown in the table, a weak dependence between the HOMO–LUMO energy gap and the position of the substituents can be found. The complexes with 4,4′- or 5,5′-substitution have a narrower energy gap than the unsubstituted (2,2′-bpy)-complex of ruthenium while substitution at the 3,3′- or 6,6′-positions leads to larger energy differences.

IR behaviour of (*n*,*n*′-L$_2$-2,2′-bipy)RuCl$_2$(CO)$_2$-type complexes were analysed by experimental or theoretical methods, concentrating on the carbonyl stretching frequencies. The frequency of the carbonyl stretching depends on the strength of the C–O bond: the lower the wavenumber, the stronger the interaction between the carbon and oxygen atoms. Thus, the changes in electron density in the sphere of central metal alter the π-back bonding leading to changes in C–O bond strength. The electronic character of the bipyridine ligand system plays a significant role in electron density of ruthenium, and it can be manipulated by varying the substituents. Electron-withdrawing groups shift the frequencies slightly upwards, while electron-donating substituents do the opposite [7]. The frequency analyses for alkoxycarbonyl substituted ruthenium bipyridine complexes were carried out in this work to clarify the role of the substituent position in carbonyl stretching frequency. Both experimental and theoretical vibration studies indicate that the position of the carbonyl peak in the IR-spectrum is nearly independent of substitution site. Alkoxycarbonyl substituent posses very similar effects regardless of the position in the bipy ring; as electron withdrawing groups they shift slightly the frequency of CO-stretching peaks to higher wave numbers in compared to the (2,2′-bpy)RuCl$_2$(CO)$_2$. Thus, the basic influence on the CO vibration is due to electron withdrawing character of the substituents and the electron density in the sphere of ruthenium does not change significantly when the substituent position is changed.

4. Conclusions

The effects of the alkoxycarbonyl substituent positions were studied by computational and experimental methods for complexes with *n*,*n*′-dialkoxycarbonyl substituted bipyridines and the position was found to have a strong effect on the character of the complexes. The relative energies of the complexes showed clear steric effects caused by the substituent positions. Alkoxycarbonyl groups at the 3,3′- and 6,6′-positions led to the structural distortion and decreased stability. When the alkoxycarbonyls were placed at the 4,4′- or 5,5′-positions no severe distortion was observed and the stabilities of the molecules were found to be considerably better than in the case of sterically strained complexes. The electrochemical character of the ruthenium complex i.e. HOMO–LUMO energy gaps were also observed to be dependent on substituent position.

The variation of the substituent position on a bipyridine ring system offers a controlled way to modify the properties of the complexes. Computational methods provide a useful tool for complex designing; the

Table 5
The energy differences ΔE (HOMO–LUMO) and IR data for the carbonyl stretching of the (n,n'-alkoxycarbonyl-2,2′-bpy)$RuCl_2(CO)_2$ complexes

Isomer	n,n'	Alkoxy	ΔE (eV)	Theoretical (cm^{-1})		Experimental (cm^{-1}) [a]	
				$_{as}$(CO)	$_{s}$(CO)	$_{as}$(CO)	$_{s}$(CO)
trans(Cl) [19]	–	–	3.13	2005	2066	2003	2066
trans(Cl)	3,3′	Methoxy	2.97	2008	2069		
trans(Cl)	4,4′	Methoxy	2.78	2009	2068	2010	2068
trans(Cl)	5,5′	Methoxy	2.58	2011	2070		
trans(Cl)	5,5′	Ethoxy	2.60	2010	2070		
trans(Cl)	6,6′	Methoxy	3.16	2011	2082		
Chelate		Methoxy	3.20	2004	2067	2012	2073
cis(Cl) [19]	–	–	3.11	2004	2068	2003	2067
cis(Cl)	3,3′	Methoxy	2.83	2005	2069		
cis(Cl)	4,4′	Methoxy	2.80	2007	2071		
cis(Cl)	5,5′	Methoxy	2.58	2006	2070	2010	2070
cis(Cl)	5,5′	Ethoxy	2.60	2006	2070	2009	2069
cis(Cl)	6,6′	Methoxy	3.11	2012	2072	2014	2073

[a] Measured in CH_2Cl_2.

compounds with unfavourable properties can be left out without sometimes long experimental work. The modifiability can be exploited in design of novel ruthenium bipyridine based catalysts and photosensitisers, in which applications the substituents of the bipyridine play a significant role.

5. Supplementary material

Crystallographic data for the structural analysis have been deposited with the Cambridge Crystallographic Data Centre, CCDC nos. 167184, 167185–167187 for complexes **1**, **3**–**5**, respectively. Copies of these data may be obtained free of charge from The Director, CCDC, 12 Union Road, Cambridge CB2 1EZ, UK (Fax: +44-1223-336033; e-mail: deposit@ccdc.cam.ac.uk or www: http://www.ccdc.cam.ac.uk).

Acknowledgements

Financial support by a grant from the Academy of Finland (M.H.) is gratefully acknowledged.

References

[1] See for example: (a) K. Toyohara, H. Nagao, T. Adachi, T. Yoshida, K. Tanaka, Chem. Lett. (1996) 27;
(b) D. Choudhury, D.J. Cole-Hamilton, J. Chem. Soc. Dalton Trans. (1982) 1885;
(c) H. Ishida, K. Tanaka, M. Morimoto, Organometallics 5 (1986) 724;
(d) J.G. Haasnoot, W. Hinrichs, O. Weir, J.G. Vos, Inorg. Chem. 25 (1986) 4140.

[2] (a) C. Ungermann, V. Landis, S.A. Moya, H. Cohen, H. Walker, R.G. Pearson, R.G. Rinker, P.C. Ford, J. Am. Chem. Soc. 101 (1979) 5922;
(b) D.C. Gross, P.C. Ford, Inorg. Chem. 21 (1982) 1704;
(c) D.C. Gross, P.C. Ford, J. Am. Chem. Soc. 107 (1985) 585;
(d) U. Kiiski, T. Venäläinen, T.A. Pakkanen, O. Krause, J. Mol. Catal. 64 (1991) 163;
(e) P. Hirva, T. Venäläinen, T.A. Pakkanen, J. Catal. 148 (1994) 722;
(f) M. Haukka, T. Venäläinen, M. Kallinen, T.A. Pakkanen, J. Mol. Catal. 136 (1998) 127.

[3] (a) L.K. Johnson, C.M. Killian, M. Brookhart, J. Am. Chem. Soc. 117 (1995) 64;
(b) D.G. Musaev, R.D.J. Froese, M. Svensson, K. Morokuma, J. Am. Chem. Soc. 119 (1997) 367;
(c) L. Deng, P. Margl, T. Ziegler, J. Am. Chem. Soc. 119 (1997) 6177;
(d) T. Schleis, J. Heinemann, T.P. Spaniol, R. Mülhaupt, J. Okuda, Inorg. Chem. Commun. 1 (1998) 431;
(e) D. Pappalardo, M. Mazzeo, C. Pellechia, Macromol. Rapid Commun. 18 (1997) 1017;
(f) C.M. Killian, L.K. Johnson, M. Brookhart, Organometallics 16 (1997) 2005;
(g) T. Schleis, T.P. Spaniol, J. Okuda, J. Heinemann, R. Mülhaupt, J. Organomet. Chem. 569 (1998) 159;
(h) L. Deng, P.M. Margl, T. Ziegler, J. Am. Chem. Soc. 119 (1997) 1094;
(i) D.G. Musaev, M. Svensson, K. Morokuma, S. Strömberg, K. Zetterberg, P.E.M. Siegbahn, Organometallics 16 (1997) 1933;
(j) D.G. Musaev, R.D.J. Froese, K. Morokuma, New J. Chem. 21 (1997) 1269;
(k) S. Strömberg, K. Zetterberg, P.E.M. Siegbahn, J. Chem. Soc. Dalton Trans. (1997) 4147;
(l) R.D.J. Froese, D.G. Musaev, K. Morokuma, J. Am. Chem. Soc. 120 (1998) 1581.

[4] S. Luukkanen, P. Homanen, M. Haukka, T.A. Pakkanen, A. Deronzier, S. Chardon-Noblat, D. Zsoldos, R. Ziessel, Appl. Catal. A 185 (1999) 157.

[5] T.-J.J. Kinnunen, M. Haukka, T.T. Pakkanen, T.A. Pakkanen, J. Organomet. Chem. 613 (2000) 257.

[6] K. Kalyanasundaram, M. Grätzel (Eds.), Photosensitization and Photocatalysis Using Inorganic and Organometallic Compounds, Kluwer Academic Publishers, Dordrecht, 1993, p. 113.

[7] T.-J.J. Kinnunen, M. Haukka, M. Nousiainen, A. Patrikka, T.A. Pakkanen, J. Chem. Soc. Dalton Trans. (2001) 2649.

[8] P.N.W. Baxter, PhD Thesis, University of Kent, 1990.

[9] C.P. Whittle, J. Heterocycl. Chem. 14 (1977) 191.

[10] Collect Data Collection Software, Nonius B.V., 1997–2000.

[11] Z. Otwinowski, W. Minor, in: C.W. Carter Jr., R.M. Sweet (Eds.), Processing of X-ray Diffraction Data Collected in Oscillation Mode, Methods in Enzymology, vol. 276, Macromolecular Crystallography, Part A, Academic Press, New York, 1997, pp. 307–326.

[12] G.M. Sheldrick, SHELXTL PLUS, release 4.11/V, Siemens Analytical Instruments, Inc., Madison, WI, 1990.

[13] G.M. Sheldrick, SHELXS-97, Program for Crystal Structure Determination, University of Göttingen, 1997.

[14] L.J. Farrugia, J. Appl. Crystallogr. 32 (1999) 837.

[15] P.T. Beurskens, G. Beurskens, R. de Gelder, S. Garcia-Granda, R.O. Gould, R. Israel, J.M.M. Smits, The DIRDIF-99 program system, Crystallography Laboratory, University of Nijmegen, The Netherlands, 1999.

[16] G.M. Sheldrick, SHELXL-97, Program for Crystal Structure Refinement, University of Göttingen, 1997.

[17] S. Huzinaga (Ed.), Gaussian Basis Sets for Molecular Calculations, Physical Sciences Data 16, Elsevier, Amsterdam, 1984.

[18] M.J. Frisch, G.W. Trucks, H.B. Schlegel, P.M.W. Gill, B.G. Johnson, M.A. Robb, J.R. Cheeseman, T. Keith, G.A. Petersson, J.A. Montgomery, K. Raghavachari, M.A. Al-Laham, V.G. Zakrzewski, J.V. Ortiz, J.B. Foresman, J. Cioslowski, B.B. Stefanov, A. Nanayakkara, M. Challacombe, C.Y. Peng, P.Y. Ayala, W. Chen, M.W. Wong, J.L. Andres, E.S. Replogle, R. Gomperts, R.L. Martin, D.J. Fox, J.S. Binkley, D.J. Defrees, J. Baker, J.P. Stewart, M. Head-Gordon, C. Gonzalez, J.A. Pople, Gaussian, Inc., Pittsburgh, PA, 1995.

[19] M. Haukka, J. Kiviaho, M. Ahlgrén, T.A. Pakkanen, Organometallics 14 (1995) 825.